Structural and dielectric properties of Cobaltacarborane Composite Polybenzimidazole Membranes as solid polymer electrolytes at high temperature

Isabel Fuentes[a], *Andreu Andrio,*[b] *Abel García-Bernabé,*[c] *Jorge Escorihuela* [c] *Clara Viñas,*[a] *Francesc Teixidor,*[a,*] *Vicente Compañ*[c,*]

[a] Institut de Ciència de Materials de Barcelona, ICMAB-CSIC, Campus Universitat Autònoma de Barcelona, 08193 Bellaterra, Barcelona, Spain. E-mail: Teixidor@icmab.es; Tel: 34 93 580 18 53, ext 247.

[b] Departamento de Física Aplicada, Universidad Jaume I, Avda. Sos Baynat s/n, 12071 Castellón de la Plana, Spain.

[c]Escuela Técnica Superior de Ingenieros Industriales. Departamento de Termodinámica Aplicada, Universitat Politècnica de València, Camino de vera s/n, 46022- Valencia, Spain. E-mail: vicommo@ter.upv.es; Fax: +34 96 387 79 24; Tel: +34 96 387 93 28.

Corresponding author:

[*,a]*E-mail: teixidor@icmab.es*

[*,c]*E-mail: vicommo@ter.upv.es*

KEYWORDS: Polybenzimidazole, Metallacarboranes, Composite membrane, Electrochemical Impedance Spectroscopy, Conductivity.

ABSTRACT

The conductivity of a series of composite membranes, based on polybenzimidazole (PBI) containing the metallacarborane salt M[Co($C_2B_9H_{11}$)$_2$], M[COSANE] and tetraphenylborate, M[B(C_6H_5)$_4$], M[TPB] both anions having the same number of atoms and the same negative charge have been investigated. Different cations (M = H^+, Li^+ and Na^+) have been studied and the composite membranes have been characterized by water uptake, swelling ratio, ATR FT-IR, thermogravimetric analysis and electrochemical impedance spectroscopy to explore the dielectric response and ion dynamics in composite membranes. Our results show that conductivity increases with temperature increase and it is higher for H^+ than for Li^+ and Na^+ for all temperatures under study. The mobility of Li^+ is greater in $[COSANE]^-$ than in $[TPB]^-$ composites PBI@ membranes while for Na^+ is the opposite. The temperature dependence of the conductivity of the composite was followed by a typical Arrhenius behaviour with two different regions: 1) between 20 and 100 ºC, and 2) between 100 and 150 ºC. Using the analysis of the electrode polarization (EP) based on the Thrukhan theory we have calculated the ionic diffusion coefficients and the density of carriers. From double logarithmic plot of the imaginary part of the conductivity (σ") versus frequency in the complete range of temperatures studied we have determined for each sample at each temperature, the frequency values of the onset (f_{ON}) and full development of electrode polarization (f_{MAX}), respectively, which permit to calculate the static permittivity.

1. INTRODUCTION

Fuel cells provide a sustainable and high efficient alternative to oil based technology that is responsible of the global CO_2 emissions, whose concentration in the atmosphere has been increasing significantly over the past century. The International Energy Agency (IEA) estimated in 2014 that the transportation sector accounted for 23% of the global CO_2 emissions that are responsible for the climate change.[1] Consequently, great efforts are being made on the development of novel polymer electrolyte membranes as solid low-cost and durable electrolytes, exhibiting high performance applications in the fields of rechargeable metal ion batteries,[2,3] supercapacitors,[4,5] proton-exchange membrane fuel cells (PEMFC)[6,7] and direct methanol fuel cells (DMFC).[8,9] To that end different approaches have been studied in the last few years, one of them emphasizes on the dispersion of hygroscopic metal oxide particles in acidic membranes.[10-14] To use these inorganic fillers, which may enhance both water retention and thermal stability,[15-17] it is paramount the improvement of polymer filler compatibility to hinder the formation of inorganic aggregations that is detrimental to the performance, durability and continuous operation of the devices. Another approach is based on hybrid organic-inorganic composite polymer electrolyte membranes, also known as mixed matrix membranes (MMMs),[18] which have attracted increasing attention because they can overcome the problems associated with purely organic membranes. The polymer electrolyte membrane (PEM) is restrictive to the permeability of the fuel when it is used as PEM in a direct methanol fuel cell. Consequently, MMMs when acting as a barrier to fuels, may be of potential interest in such devices because they allow the transport of protons from the anode to the cathode.

On the other hand, sandwich $M[Co(C_2B_9H_{11})_2]$ ($M = Li^+, Na^+, H^+$) (also called M[COSANE]), represented in Fig. 1, is an anionic compound, with a very low charge density, electroactive with a reversible redox process, highly stable and with many possibilities for derivatization in a stepwise fashion. Despite being a purely inorganic molecule, it has a substitution behavior comparable or superior to organic frameworks. This is why one would expect that the metallacarboranes would be adequate inorganic components for producing hybrid organic/ $M[Co(C_2B_9H_{11})_2]$ materials with innovative features.

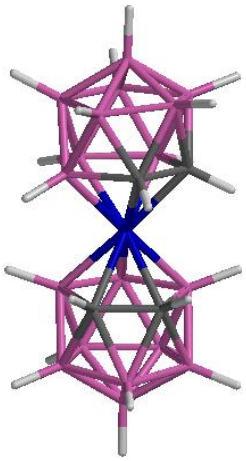

Fig. 1 Molecular representation of $[Co(C_2B_9H_{11})_2]^-$.

Just as an organic polymer fragment has hydrophobic sites and has polar points, depending on the substituents, M[COSANE] has hydrophobic characteristics, but also polar behavior as has been demonstrated by its ability to produce vesicles, micelles and lamellae. These properties, effectively make these anionic molecules attractive for producing hybrid organic-inorganic composites for any desired application.

Organic-inorganic hybrid materials between $[COSANE]^-$ and polypyrrole or polythiophene have been reported. In the pyrrole polymerization process, a positively charged polymer is produced that is doped with the reversible redox active $[Co(C_2B_9H_{11})_2]^-$. Indeed, the PPy/ $[Co(C_2B_9H_{11})_2]^-$ represents an excellent example of the integration at the molecular level, being a genuine example of hybrid materials.

These anions display strong non-bonding interactions with themselves and with polymers, inducing properties in addition to the individual characteristics of the components. These results and others led to the belief that these metallacarboranes can be useful components of MMMs and molecular electronics for a wide range of potential applications.

Earlier we studied the temperature dependence of the ionic conductivity of $M[Co(C_2B_9H_{11})_2]$, and $M[B(C_6H_5)_4]$ M = Li^+, Na^+ and H^+ with the aim to compare the results of the dc-conductivity.[19] It is to be noticed that the anions in both salts have the same number of atoms. We have observed that the conductivity of Na^+ ions in the metallacarborane is larger or at least comparable with the one with Li^+. This suggests that they may have good opportunities for their use in a new generation of batteries incorporating sodium ions. Furthermore, we have found that the dc-conductivity is higher

for M[COSANE] M= H^+, Li^+, Na^+, than for M'[TPB], M'= Li^+, Na^+, however the dc-conductivity for Li^+ and Na^+ salts is opposite in the two anions. It is higher for Na[COSANE] than for Li[COSANE] whereas it is higher for Li[TPB] than for Na[TPB]. The conductivity comparison between Li[COSANE] and Na[COSANE] indicates that the change in cation either Li^+ or Na^+ is insignificant in all the range of temperatures, but the relaxation time increases when the cations are protons. This indicates that the counter ions affect the frequency at which the polarization starts to be significant in the system. These results express that the diffusivity of ions in $[COSANE]^-$ is higher than in $[TPB]^-$.

To this end, in this work we want to explore the possibilities offered by M[$Co(C_2B_9H_{11})_2$] (M = Li^+, Na^+, H^+) M[COSANE] and M'[$B(C_6H_5)_4$] (M' = Li^+, Na^+) M'[TPB], to produce hybrid organic-inorganic composite membranes of higher conductivity, when the hydration is present in its structure. We want also to know what will be the behaviour without hydration, at temperatures up to 100 ºC, when these powders are in a polymer matrix as MMMs. This opens an excellent possibility for their use in a new generation of batteries incorporating sodium ions, as PEMFC and DMFC, to work at moderate and high temperatures in a polymer doped to acquire an acidic state.

Phosphoric acid-doped PBI membranes are gaining increasing interest in the last decades among other type of polymeric membranes for the high temperature range (120-200 °C).[18] In this regard, PBI membranes are becoming excellent candidates to replace typical perfluorosulfonic acid polymer electrolytes, such as Nafion,[20] which are unsuitable for operating at high temperature due to the decrease of proton conductivity around 80 °C.[21] Although phosphoric acid doping enhances proton conductivity in PBI membranes, its use has some drawbacks regarding environmental issues associated to phosphoric acid leaking and acid evaporation around 160 °C, which produces an important decrease of proton conductivity. Consequently, significant efforts have been directed towards the search and development of alternative approaches to enhance PBI proton conductivity. In this regard, the most common alternatives are based on the grafting of phosphonic acid to PBI polymer[22] or the addition of doping agents, such as graphene or silica.[23] Añadir las siguientes referencias: (1) S. Singha and T. Jana, ACS Appl. Mater. Interfaces, 2014, 6, 21286–21296. (2) S. R. Kutcherlapati, R. Koyilapu and T. Jana, J. Polym. Sci. A Polym. Chem. 2018, 56, 365-375. (3) S. Maity, S. Singha and T. Jana, Polymer 2015, 66, 76-85. J. L. Reyes-Rodriguez, J. Escorihuela, A. García-

Bernabé, E. Giménez, O. Solorza-Feria and V. Compañ, RSC Adv., 2017, 7, 53481-53491.

In this work we have synthesized and characterized PBI@M[COSANE] and PBI@M[TPB] composite membranes with different ions (H^+, Li^+ and Na^+). To do so, detailed investigations of ATR FT-IR, Thermogravimetric analysis (TGA), water uptake, swelling ratio and electrochemical impedance spectroscopy (EIS) have been done. The dielectric properties and conductivities of MMMs membranes prepared from (a) M[COSANE], (M = H^+, Li^+, Na^+) and (b) M'[TPB], (M' = Li^+, Na^+) with comparable thicknesses have been studied from 20 to 160 ºC. The experimental procedure has been done at the extremes: under fully hydrated and in dry conditions. The differences observed are discussed. The results obtained allow us to conclude that the composite membranes may have interesting transport properties as solid electrolytes for batteries, supercapacitors and fuel cell applications.

2. EXPERIMENTAL

2.1. Materials. Polybenzimidazole (PBI) with a molecular weight of 65000 $g \cdot mol^{-1}$ was purchased from Danish Power Systems. LiCl, N,N-dimethylacetamide (DMAc) 99.8% and Na[TPB] were purchased from Sigma-Aldrich. Li[TPB], H[COSANE], Na[COSANE] and Li[COSANE] were synthesized from commercial samples, as previously described.[19]

2.2. Preparation of membranes.

2.2.1. Preparation of PBI solution. 1g of LiCl as a stabilizer was dissolved in 100 g of DMAc with vigorous stirring to give a 1 wt. % solution. Next, 10 g of PBI powder was dissolved in 100 g of the 1 wt. % LiCl of previous solution and was heated under reflux at 120 °C for 6 h to form a 10 wt. % PBI solution.

2.2.2. Preparation of PBI composite membranes.

Composite PBI membranes were prepared by casting method. The proper amount of metallacarborane or conventional tetraphenylborate (10 mg) was dissolved in 2 g of the previous PBI solution under vigorous stirring to give the composite PBI solution of 5 wt. % of metallacarborane or tetraphenylborate. This solution was cast onto a glass plate and dried at 80 °C for 8 h, then was dried at 160 °C for 16 h to remove residual DMAc solvent. The membranes were then peeled off the glass plate and finally dried under vacuum at 140 °C for 10 min.

2.3 Characterization of the composite membranes.

2.3.1. Fourier transform infrared spectroscopy (FTIR) analysis. Fourier transform infrared spectra (FTIR) of membranes were recorded using a MIRacle single-reflection ATR diamond/ZnSe accessory in a Jasco FT-IR 6200 spectrometer between 500 and 4000 cm^{-1} with a 4 cm^{-1} resolution and an Attenuated Total Reflectance (ATR) cell. Backgrounds were acquired before every third samples.

2.3.2 Water uptake and swelling ratio. Samples were initially dried in vacuum at 100 °C for 24 h. Next, 2 × 2 cm membranes were immersed in deionized water at room temperature for 2 days and then wiped with absorbent paper to remove surface water. The water uptake and swelling ratio of the membrane were calculated according to the following equations

$$\text{Water uptake}(\%) = \frac{W_{wet} - W_{dry}}{W_{dry}}$$

$$\text{Swelling ratio}\ (\%) = \frac{L_{wet} - L_{dry}}{L_{dry}}$$

where W_{wet} and W_{dry} are the weight of membrane after and before water absorption, respectively; L_{wet} and L_{dry} are the thickness of the wet and dry membranes, respectively. Three independent tests were conducted and the average values were calculated.

2.3.3. Thermogravimetric analysis (TGA). Thermal stability of membranes was characterized by thermogravimetric analysis on a Mettler-Toledo TGA/SDTA 851 apparatus. All samples (5-10 mg) were weighed in zirconia crucibles and were heated in a nitrogen flow (100 mL· min^{-1}) at a heating rate of 10 °C·min^{-1} from 30 to 800 °C.

2.3.4. Electrochemical impedance spectroscopy (EIS). Impedance measurements were carried out on composite PBI films at several temperatures in the range 20 ºC to 200 ºC and a frequency window of $10^{-1} < f < 10^{7}$ Hz. The experiments were performed with 100 mV amplitude, using a Novocontrol broadband dielectric spectrometer (Hundsangen, Germany) integrated by a SR 830 lock-in amplifier with an Alpha dielectric interface. The sample of interest was sandwiched between two gold circular electrodes coupled to the impedance spectrometer acting as blocking electrodes. The membrane-electrode assembly was annealed in the Novocontrol setup under an inert dry nitrogen atmosphere before the start of the actual measurement. During the experiment, the temperature was gradually raised from 20 to 120 ºC in steps of 10 ºC and lowered down to 20 ºC. In a subsequent experiment the temperature was increased from 20 to 200 ºC in steps of 20 ºC, and in this cycle of temperature scan the dielectric spectra were collected in each step. The measurements were carry out in wet conditions. For this, the samples previously were stored with bi-distilled water during 24 hours. Afterwards placed between two gold electrodes in a liquid parallel plate cell BDS 1308 liquid device, which was coupled to the spectrometer, and incorporating water deionized water (Milli-Q) to ensure fully hydrated state of the membranes below 100ºC and in equilibrium with its vapour above 100ºC, to simulate 100% RH atmosphere. During the conductivity measurements the temperature was kept isothermally controlled by a nitrogen jet (QUATRO from Novocontrol) with a temperature error of 0.1 ºC during every single sweep in frequency.

3. RESULTS AND DISCUSSION

3.1. Membrane preparation and physicochemical properties.

Composite PBI membranes were prepared by casting method. The proper amount of metallacarborane or conventional tetraphenylborate (5 wt. %) was dissolved in the PBI solution with DMAc under vigorous stirring to give the composite PBI solution. This solution was cast onto a glass plate and dried to give membranes of thickness around 200 μm. Fig. 2 shows a schematic representation of the composite membrane preparation.

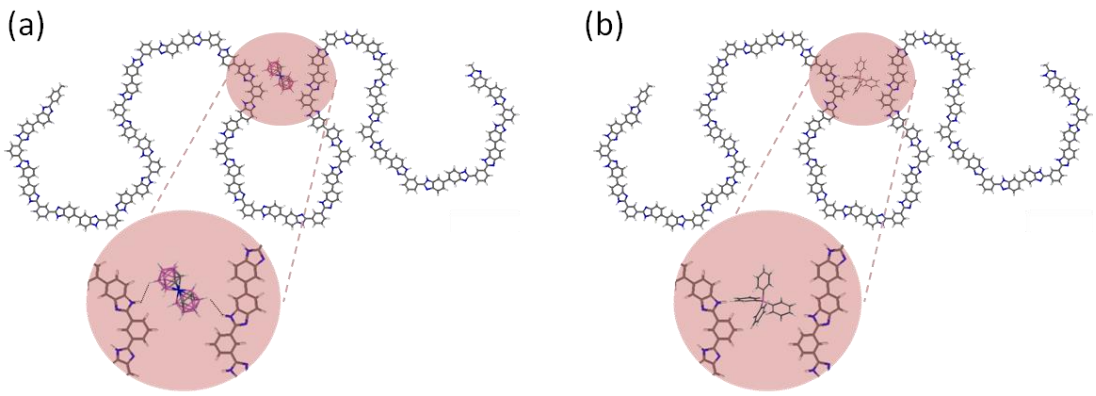

Fig. 2 Schematic representation of PBI composite membranes containing metallacarborane, $[Co(C_2B_9H_{11})_2]^-$, and tetraphenylborate, $[B(C_6H_5)_4]^-$.

Table 1 shows different physicochemical properties related to the thickness, water uptake, swelling ratio and thickness uptake from the PBI membranes containing M[COSANE] and M'[TPB] at 25 ºC.

Table 1. Membrane thickness, water uptake (at 25 °C), swelling degree and thickness uptake for PBI and PBI membranes containing different salts of the metallacarborane, $M[Co(C_2B_9H_{11})_2]$, ($M = H^+$, Li^+, Na^+), and tetraphenylborate, $M'[B(C_6H_5)_4]$ ($M' = Li^+$, Na^+) (5% wt).

Sample	Thickness (μm)	Water uptake (%)	Swelling ratio (%)	Thickness uptake (%)
PBI	210 ± 14	108 ± 2	53 ± 2	33 ± 2
PBI@H[COSANE]	222 ± 8	122 ± 2	58 ± 2	41 ± 2
PBI@Na[COSANE]	218 ± 7	118 ± 2	56 ± 2	38 ± 2
PBI@Li[COSANE]	214 ± 10	136 ± 2	62 ± 2	40 ± 2
PBI@Na[TPB]	209 ± 9	127 ± 2	60 ± 2	43 ± 2
PBI@Li[TPB]	203 ± 5	134 ± 2	63 ± 2	37 ± 2

3.2. Fourier transform infrared spectra

Infrared spectroscopy is very informative in this case because $[COSANE]^-$ has B-H bands in the region near 2500 cm^{-1} in which no other common frequency appears. Fig. 3 shows the FT-IR spectra of the different composite membranes of metallacarboranes (M[COSANE] ($M = Li^+$, Na^+, H^+)) and tetraphenylborate

(M'[TPB] (M' = Li^+, Na^+) in the range of 4000–600 cm^{-1}. The pristine PBI membrane showed a broad peak around 3500–3200 cm^{-1} due to the N–H stretching and bands at 1607 cm^{-1} and 1421 cm^{-1}, which are associated with C=N and C–N stretching vibrations, respectively. The incorporation of the different $[COSANE]^-$ salts in the polymer matrix was confirmed by the presence of an intense band at 2525 cm^{-1}, due to the B–H stretching. In the case of PBI membrane containing 5 wt. % of tetraphenylborate salts, the infrared spectra show sharp bands near the region of 3000 cm^{-1} due to C-H stretching of the four phenyl groups (see Figure S1, in electronic supplementary information).

3.3. Thermal analysis and mechanical properties.

To guarantee an efficient proton transport, it is required that ideal polymer electrolyte membranes exhibit high thermal stability at elevated temperatures. The thermal properties of PBI-based membranes with metallacarborane salts and tetraphenylborate salts (5 wt. %) were analyzed by TGA under N_2 atmosphere (Fig. 3). For the pristine PBI membrane, about 5% loss occurs in the range of temperature from 50 to 350 °C, basically due to the dehydration of absorbed water molecules and DMAc. The polymeric backbone degradation occurs around 710 °C. All PBI composite membranes containing 5 wt. % of metallacarborane showed high thermal stability up to 250 °C, with a weight loss of 2-4% depending on the cation, being PBI@H[COSANE] and PBI@Na[COSANE] slightly more stable than PBI@Li[COSANE]. However, above 200 °C, they posses lower therml stability compared to that of the pristine PBI membrane, in particular for TPB-based composite membranes. Following the initial decomposition stage, composite membranes retained 85-90% weight at 450 °C. Among all the metallacarborane composite membranes under study, PBI@H[COSANE] remained with 87% weight at 600 °C, slightly less than pure PBI membrane. A final decomposition stage was observed after 600 °C and composite membranes remained with 74-81% weight at 800 °C. For PBI membranes containing 5 % wt of tetraphenylborate salts, thermal stability was lower compared to composite membranes containing metallacarborane salts. In this regard, membranes PBI@Li[TPB] and PBI@Na[TPB] present a degradation near 180 °C, with a 25% weight loss around 450 °C. The composite membrane containing Na[TPB] was slightly more thermally stable after 450 °C, starting another degradation stage around 600 °C.

Finally, after several decomposition stages, composite membranes containing Li[TPB] and Na[TPB], remained with 44% and 56% weight at 800 °C, respectively.

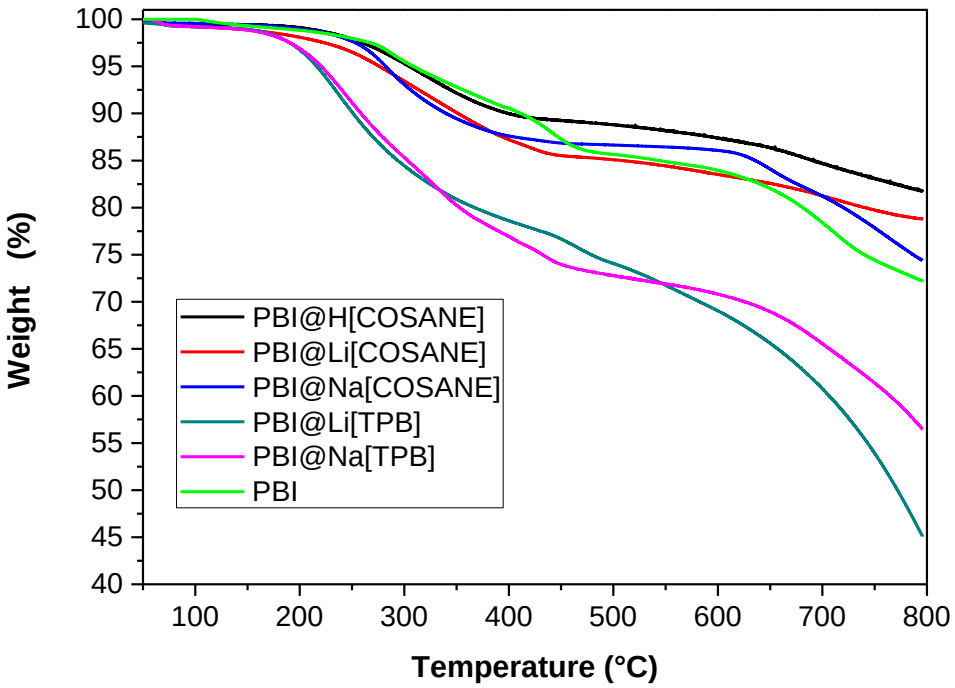

Fig. 3 TGA curves of PBI pure membrane and PBI@H[COSANE], PBI@Na[COSANE], PBI@Li[COSANE], PBI@Li[TPB] and PBI@Na[TPB] composite (5 % wt) PBI membranes under N_2 atmosphere.

3.4. Electrochemical impedance spectroscopy (EIS).

3.4.1. Temperature dependence of conductivity

Impedance spectroscopy measurements were carried out on composite PBI samples in the temperature range 25 °C to 200 °C and in the frequency range 0.1 Hz to 10 MHz to study the dielectric and ac conductivity behavior. The dielectric analysis of the polymeric membranes can be illustrated by complex permittivity, $\varepsilon(\omega)^* = \varepsilon'(\omega) - j\varepsilon''(\omega)$, where $\varepsilon'(\omega)$ and $\varepsilon''(\omega)$ are the real and imaginary parts of the frequency dependent permittivity due to the applied electric field, and j the imaginary unity ($j^2 = -1$).

The relation between the complex dielectric permittivity ($\varepsilon^*(\omega,T)= \varepsilon'(\omega,T) -\varepsilon''(\omega,T)$) and the complex conductivity, $\sigma^*(\omega,T)$, is given by:

$$\sigma^*(\omega,T) = j\varepsilon_0\omega\varepsilon^*(\omega,T) \qquad (1)$$

which can be expressed in the real and imaginary part as follows:

$$\sigma' = \varepsilon_0\omega\varepsilon'' \qquad (2)$$

$$\sigma'' = \varepsilon_0\omega\varepsilon' \qquad (3)$$

where ε_0 represents the vacuum permittivity and ω the angular frequency of the applied electric field ($\omega = 2\pi f$). The conductivity σ´ is characterized by a plateau regime that directly yields the dc conductivity. In this regime σ'(ω) is identical to the bulk dc conductivity σ_{dc} (i.e. σ_0), and the conductivity of the composite PBI should be determined, reflecting long-range ion transport. Typical curves showing the variation of the real part of conductivity for all the samples in all the interval of temperatures is show in Fig. 4.

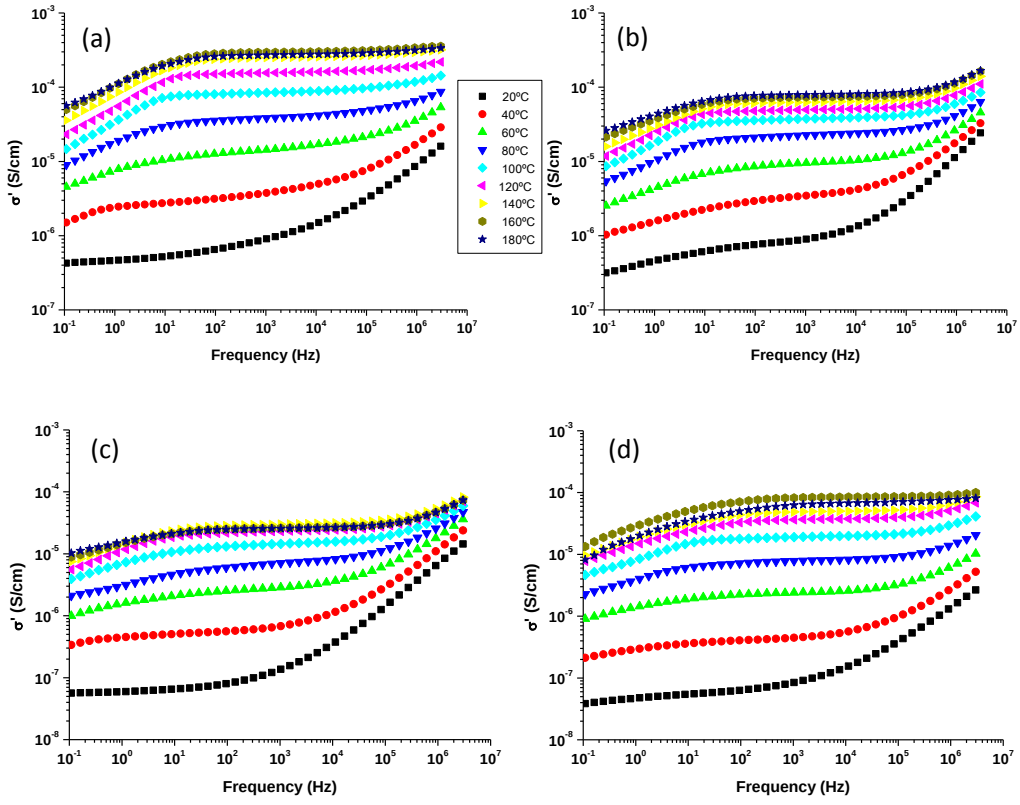

Fig. 4 Double logarithmic plot of the real part of the conductivity, σ', versus frequency for the samples a) PBI@H[COSANE], b) PBI@Li[COSANE], c) PBI@Na[COSANE] and d) PBI@Li[TPB] for several temperatures: 20 ºC (■), 40 ºC (●), 60 ºC (▲), 80 ºC(▼), 100 ºC (◆), 120 ºC(◀), 140 ºC (▶), 160 ºC (⬢) and 180 ºC (✶).

A similar behaviour has been observed for the sample PBI@Na[TPB] (See Fig. S1). On the other hand, after plateau regime at very higher frequencies, σ'(ω) increases with increasing frequency. In this region, the subdiffusive conductivity (SD) is given, and it corresponds to the dispersive regime providing information of localized movements of ions into the membranes.[24,25] At lower frequencies, it is observed that σ' decreases from σ_0 and this is due to electrode polarization that results from blocking the charge carriers at the electrodes.[26]

On the other hand, the plot of tan δ vs. frequency reaches a maximum at a characteristic frequency $\omega_c=2\pi f_c$, at which dispersion sets in and turns into a power law at higher frequencies region. From these spectra we have determined the value of the conductivity at the frequency where the loss tangent, (tan δ), reach the maximum, such is showed in Fig. 5.

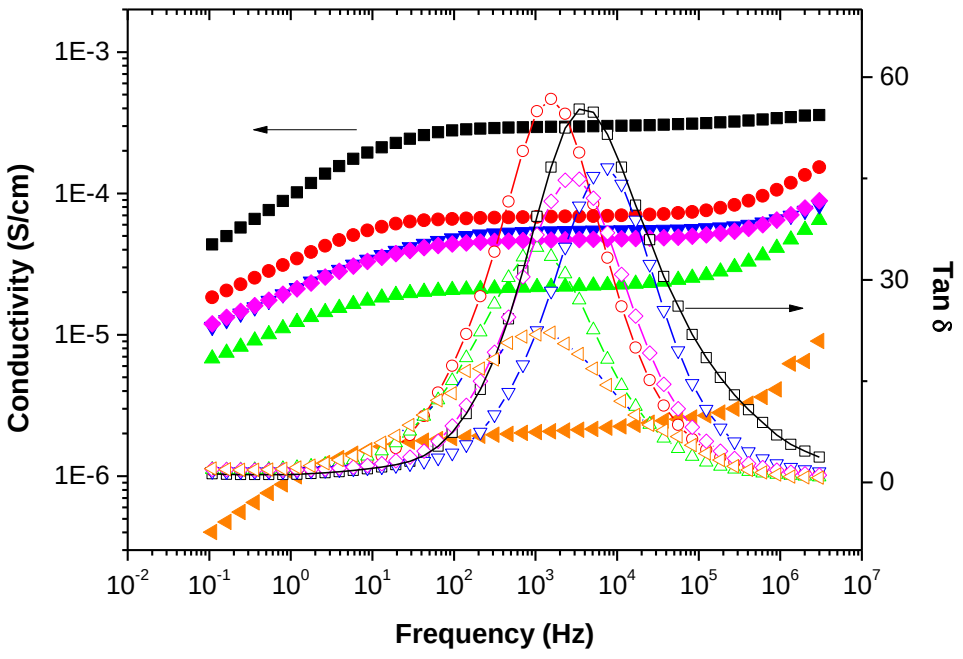

Fig. 5 Double logarithmic plot of the real part of the conductivity σ' versus frequency for all samples at 150 ºC, and variation of tan δ vs. frequency for the same samples at 150 ºC. σ(PBI@H[COSANE]) (■), σ(PBI@Na[COSANE]) (▲), σ(PBI@Li[COSANE]) (●), σ(PBI@Na[TPB]) (◆), σ(PBI@Li[TPB]) (▼). In open symbols (identical colours) we plot tan δ for the same membranes. For comparison we are also plotted the double logarithmic plot of the real part of the conductivity σ'(◀) and Tan δ (◁) versus frequency for pristine PBI membrane at 150 ºC.

Combining the plots shown in Fig. 4 and 5 we have determined the conductivities of the samples in all the range of temperatures, taking the cut-off frequency as the onset of electrode polarization (EP) which we define as the maximum in tan δ. Thereby the corresponding value of $f_{max}^{\tan\delta}$ has been taken to determine the dc-conductivity of the samples. For all temperatures studied, our results show that conductivity for all composites raises with temperature increase following the order σ(PBI@H[COSANE]) > σ(PBI@Na[COSANE]) > σ(PBI@Li[COSANE]) > σ(PBI@Na[TPB]) > σ(PBI@Li[TPB]). A comparison between the conductivities of the composite samples with pristine PBI (see Fig. 5) shows that conductivities of composites at 150 ºC are higher than pristine PBI membranes, between one to two orders of magnitude depending on the type of ion. For the other temperatures the results are similar.

Fig. 6 shows the conductivity values for all samples as a function of temperature. From this plot, we can see that all samples follow a typical Arrhenius behaviour with two different behaviours: one in the interval of temperatures between 20 and 100 ºC, where the conductivity increases with increasing temperature. For temperatures above 100 ºC, in case of pristine PBI membrane, the conductivity strongly begins to fall down may be due to the hydration of the membrane. However, for composite membrane we observe a second behaviour between 100 and 150 ºC where the conductivity tends to increase with different slope compared to the first interval up to 150 ºC. At temperatures above 150 ºC, in composite membranes, conductivities decrease with increasing temperature. This is possible due to the solvent evaporation temperature used in membranes preparation. The evaporation temperature of solvent (DMAc) is about 160 ºC and could be this the reason by which above this temperature the conductivity of the membranes diminish. However, for the sample PBI@Na[TPB] we observe an increase in conductivity at temperatures

above 160 ºC. Similar results have been found in proton exchange membranes based on semi-interpenetrating polymer networks of polybenzimidazol and perfluorosulfonic acid polymer with hollow silica spheres(HPSS) as additive.[27] The values of the activation energy for each interval are collected in Table 2.

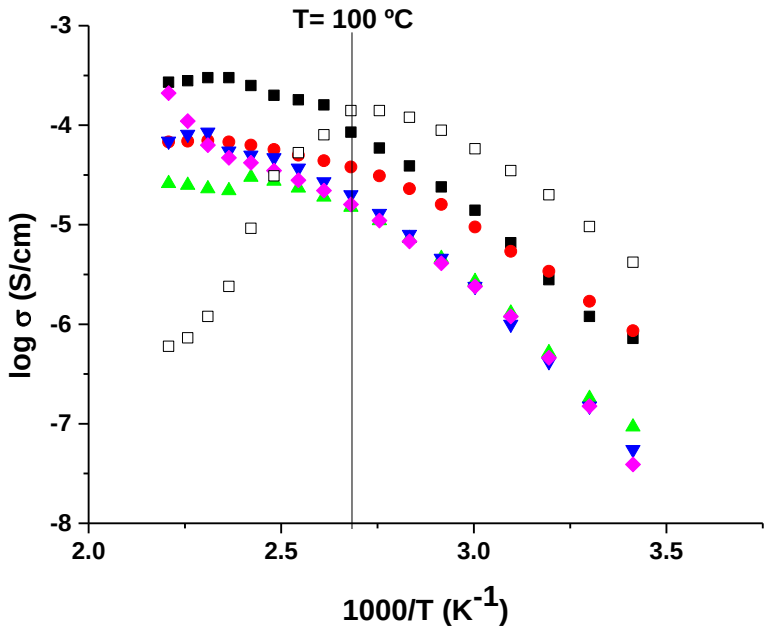

Fig. 6 Temperature dependence of conductivity obtained from Bode diagram at frequency where tan δ reach the maximum. (PBI@H[COSANE]) (■), (PBI@Na[COSANE]) (▲), (PBI@Li[COSANE]) (●), σ(PBI@Li[TPB]) (▼), (PBI@Na[TPB]) (◆). We can see two different behaviours separate by two temperatures intervals from 20 to 100 ºC and from 100 to 150 ºC. For comparison the results found for PBI@ pristine membranes is also plotted and PBI (□).

Table 2. Activation energy values for all the membranes.

Membrane	E_a (kJ/mol) T ∈[20 ºC-100 ºC]	E_a (kJ/mol) T ∈[100 ºC-150 ºC]
PBI@H[COSANE]	24.7±0.7	5.6±0.1
PBI@Li[COSANE]	19.1±0.8	3.9±0.4
PBI@Na[COSANE]	26.1±1.2	5.2±0.3
PBI@Li[TPB]	29.5±0.9	6.1±0.6
PBI@Na[TPB]	29.1±1.6	7.3±0.3
PBI	20,5±2.3	-

As expected, all values found for the composite membranes are higher than the values found for the powders where the activation energies were E_{ac}H[COSANE] = 19.9 kJ/mol > E_{ac}Na[COSANE] = 18.0 kJ/mol > E_{ac}Li[COSANE] = 14.8 kJ/mol, however when $[COSANE]^-$ is replaced by $[TPB]^-$, then the activation energy was E_{ac}Li[TPB] = 27.2 kJ/mol and E_{ac}Na[TPB] = 21.3 kJ/mol.[19] These values are smaller than the activation energy found in Poly(ethylene oxide)-based sulfonated ionomer with Li^+ (PEO^-Li^+) and Na^+ (PEO^-Na^+) where the activation energy were 25.2 and 23.4 kJ/mol, respectively.

On the other hand, these values are in agreement with those obtained for most of low molecular weight ionic liquids (ILs). The incorporation of Li^+ instead of Na^+ produces a decrease in activation energy for $[COSANE]^-$, however when the anion is $[TPB]^-$ there is hardly any variation in the activation energy.

Our results of conductivity are similar to the conductivity obtained in nanocrystalline zeolitic imidazolate framework-8 (ZIF-8),[28,29] where at 94 ºC and 98% RH was around $4.5x10^{-4}$ S/cm, but in our membranes in dry conditions the conductivity at 100 ºC is near $8.5x10^{-5}$ S/cm for the composite membrane of PBI@H[COSANE]. The activation energy values for conduction in our composites are smaller than for ZIF-8 where the values are surprisingly high, about 110 kJ/mol, more than five times these reported here in the range between ambient temperature and 100 ºC.

On the other hand, our results are quite similar to the values found for several ionic liquids HMIM-BF4 (molecular weight 254 g/mol), HMIM-Br (molecular weight 247.18 g/mol), HMIM-Cl (molecular weight 202.73 g/mol) and HMIM-I (molecular weight 312.34 g/mol), which values are near 23.3 kJ/mol and are comparable to these obtained by Rivera and Rossler for different series of imidazolium based ILs.[30,31]

As observed in Fig. 6, the dc-conductivity is higher when the anion is $[COSANE]^-$ in place of $[TPB]^-$, however the behaviour of Li^+ and **N**a^+ ions in $[TPB]^-$ present a very similar behaviour and quite similar to PBI@Na[COSANE].

Both $[COSANE]^-$ and $[TPB]^-$ are monoanionic and precisely have the same number of atoms, 45. Taking into consideration the important changes in polarity and hygroscopicity associated to the change in the cation from Li^+ to Na^+ or H^+, the presence of retained water could have an influence on the conductivity observed. In this sense the H^+ may be associated as hydronium ion resulting in a greater mobility than Li^+ and Na^+ ions.

On the other hand, a comparison between the conductivity results of our membranes and *meta*-polybenzimidazole-block-*para*-polybenzimidazole (*m*-PBI-b-*p*-PBI) block copolymers doped with phosphoric acid (PA) [Reference: Sudhangshu Maity and Tushar Jana. ACS Applied Materials & Interfaces. 2014,6 6851-6864] shows that at 160ºC our samples have conductivities around 10^{-5} S/cm while in case of PA doped block copolymer of m-PBI-b-p-PBI the coductivities increased from 0.05 to 0.11 S/cm when the molecular weight (Mn) of blocks increased from 1000 to 5500. In this work, the authors showed that the block structural motif also influences the proton conductivity despite the similar PA loading. However, studies of PA-PBI composite membranes doped with functionalized inorganic fillers such as polibenzimidazole/Silica nanocomposite electrolyte membrane showed that proton conductivity increase with filler content, but it decreased around two orders of magnitude when leaching occurred. [Reference: Shuvra Singha and Tushar Jana. ACS Appliede Materials & Interfaces. 2014, 6, 21286-21296][Reference: Chuang, S-W; Hsu, SL.-C; Hsu, C.-L; Journal Power Sources 2007, 169: 172-177.[Mustarelli P.; Quartarone E.; Grandi S; Carollo A.; Magistris A. Adv. Mater 2008, 20: 1339-1343][Lobato J, Cañizares P; Rodrigo MA; Übeda D;M Pinar FJ; Journal Power Sources 2011, 196: 8265-8271]. This increasing in conductivity is due to the self-assembled clusters of amina modified silica nanoparticles in the matrix bring in more sites for proton hopping which produce an increasing of the conductivity. However, our membranes have similar values of conductivity at higher temperatures that this kind of PA-PBI composites, after leaching of PA. Note that when the membranes are part of a MEA in the fuel cell after several test or cycles the performance will fall sharply due to loss of PA, this being the main problem of the membranes used phosphoric acid fuel cell applications (PAFCs).

3.4.2. Diffusion coefficient and free ion concentration

The analysis of the electrode polarization (EP) is based on the Thrukhan theory[32-34] that is based on the Nernst-Plank equations of the electro-diffusion applied to the case of a 1:1 charge electrolyte, where the cations and anions carry the same amount of charges. In our experimental procedure we have a sample sandwiched between two circular metallic gold plates of 10 mm diameter completely blocking the electrodes. We assume that all ions

have the same diffusivity and the thicknesses of the samples (L) are much larger than the Debye length (L_D).

From EP model, different treatments have been established to determine the mobility and concentration of charge carriers based on impedance spectroscopy measurements.[32-37] Klein et al.[37] following the method proposed by Coelho[38] have developed a model that permits to determine the ionic charge density and the ion mobility from measurements of tan δ on ionic conductors and polymeric membranes.[33,39-43] In our study we have followed a parallel study developed by Klein et al.,[37] where the complex dielectric permittivity is represented by a single Debye relaxation; we modelled the plots of tan δ versus frequency following the expression,

$$\tan\delta = \frac{\omega\tau_{EP}}{1+\frac{(\omega\tau_{EP})^2}{B}} \qquad (4)$$

Where τ_{EP} is the polarization electrodes relaxation time and B is defined as the ratio of the sample thickness, (L), to twice the Debye length, (L_D), then $B = L/2L_D$ (i.e. $B = \varepsilon_{EP}/\varepsilon_s$). Notice that Debye length is given by $L_D = \sqrt{\frac{\varepsilon_S \varepsilon_0 kT}{q^2 n_0}}$, where k is the Boltzmann constant, T the absolute temperature and n_0 the mobile charge density.

From Tan δ data fit to eqn (4) the values of parameters B and τ_{EP} have been determined for all temperatures and samples. Fig. 7 shows the different fits for the samples PBI@Li[COSANE], PBI@Na[COSANE], PBI@Li[TPB] and PBI@Na[TPB], respectively, at several temperatures (80, 100, 130 and 180 ºC). As can be seen the relaxation strength increases with temperature and such increase is higher for $[TPB]^-$ than for $[COSANE]^-$. The relaxation time of electrode polarization exhibits a behavior that cannot be described by a single Arrhenius fit, as we can see in Fig. 8 for all the samples studied. This is a clear indication that PBI@M[COSANE] and PBI@M[TPB] (M= H^+,Li^+ and Na^+) have not simple dependence with the temperature. Knowing that τ_{EP} represents the average time for an ion to travel from one electrode to another, at times longer than τ_{EP} a large quantity of ionic carriers will have built up at the electrodes and the dependence with temperature of mobilities will not present an Arrhenius behavior, as will happen with the conductivity. As can be seen in Fig. 8 the relaxation time of electrode polarization is

in the interval between 0.001 y 0.01 s for almost the entire temperature range measured. However, it is most significant the change of behavior at 120 ºC for all the samples.

On the other hand, the B values increase with increasing temperature for all samples. Table 3 shows the results found at 50, 80, 100, 130 and 180 ºC, respectively, for all the samples studied.

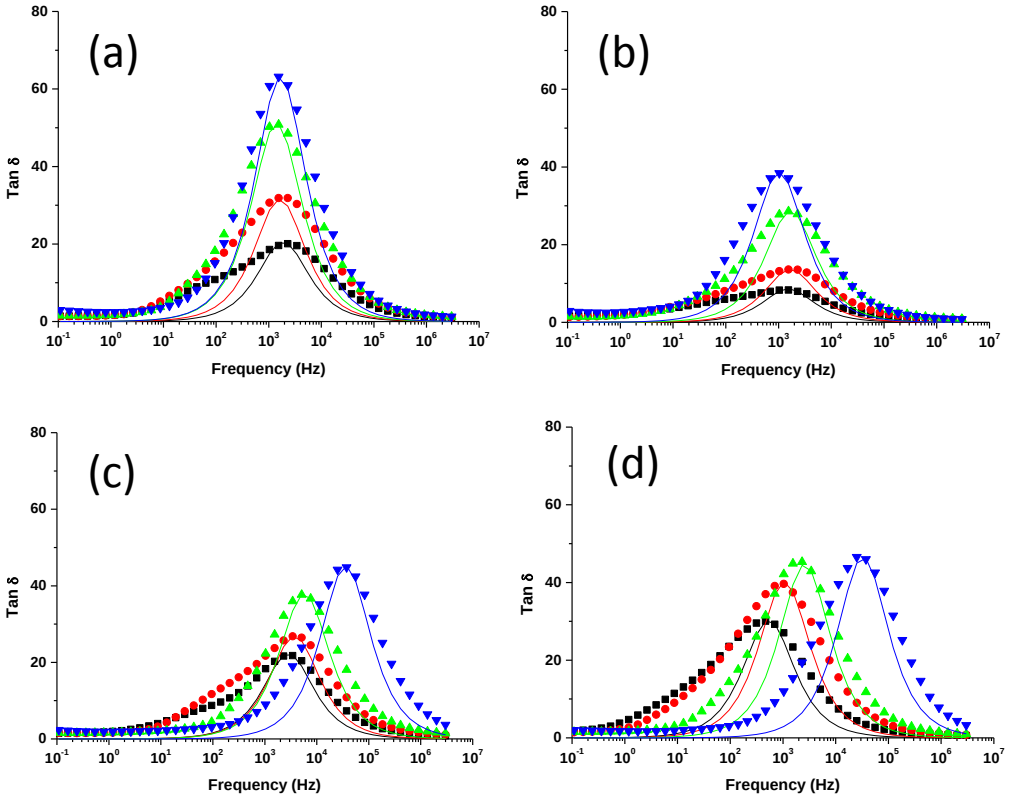

Fig. 8 Variation of loss tangent versus frequency for the samples a) PBI@Li [COSANE], b) PBI@Na[COSANE], c) PBI@Li[TPB] and d) PBI@Na[TPB], respectively. The points show the experimental results and the lines the fits using the eqn (4). The temperatures correspond to 80 ºC (■), 100 ºC (●), 130 ºC (▲) and 180 ºC (▼), respectively.

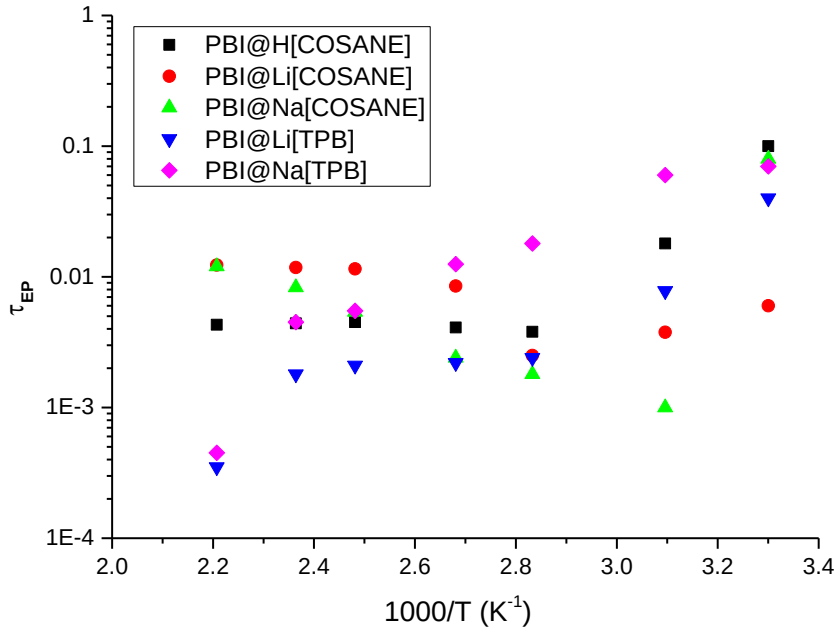

Fig. 9 Temperature dependence of the electrode polarization time τ_{EP} .

Table 3. Values found for τ_{EP} and B from fitting tan δ, diffusivity and mobile charge density for all the composites at several temperatures.

Samples	Temperature (ºC)	τ_{EP} (s)	B	Dx10^{10} (m^2/s)	Nx10^{24} (cm^{-3})
PBI@H[COSANE]	50	0.018	650	6.4	0.2
	80	0.0038	1300	0.2	0.5
	100	0.0041	3600	5.1	3.4
	130	0.0045	8500	2.0	22
	150	0.0044	10200	1.7	41
	180	0.0043	11500	1.5	44
PBI@Li[COSANE]	50	0.0038	410	48	0.02
	80	0.0025	1700	17.4	0.25
	100	0.0085	4000	2.2	3.5
	130	0.0115	10500	0.60	20
	150	0.0118	13800	0.45	34
	180	0.0123	16000	0.37	44
PBI@Na[COSANE]	50	0.0010	100	860	0.00026

	80	0.0018	300	160	0.0088
	100	0.0024	1000	36	0.085
	130	0.0054	3300	48	1.24
	150	0.0083	4200	2.4	2.0
	180	0.012	6000	1.2	5.3
PBI@Li[TPB]	50	0.0078	830	15	0.012
	80	0.0024	2000	20	0.078
	100	0.0022	2900	15	0.27
	130	0.0021	5800	7.9	1.3
	150	0.0018	8800	6.0	2.1
	180	0.00035	8200	3.3	5.1
PBI@Na[TPB]	50	0.06	1250	0.12	0.19
	80	0.018	3800	1.2	1.1
	100	0.0125	6300	1.0	3.1
	130	0.0055	8000	1.9	4.1
	150	0.0045	8300	2.2	4.9
	180	0.00045	8700	2.0	2.5

A close inspection of Table 3 shows that the relaxation time of electrode polarization presents an opposite behaviour in the case of the samples PBI@Li[COSANE] and PBI@Na[COSANE] to PBI@Li[TPB] and PBI@Na[TPB]. For $[COSANE]^-$, the relaxation time increases with increasing temperature, but for $[TPB]^-$ the relaxation time decreases for both ions just as PBI@H[COSANE]. For example, between 50 ºC and 180 ºC the τ_{EP} of PBI@Na[COSANE] increases around one order of magnitude while for PBI@Na[TPB] τ_{EP} diminishes two hundred times. If we compare the behaviour of Na^+ and Li^+ ions in PBI@M[COSANE] samples we observe that τ_{EP} increases fivefold when the ion is Li^+ than Na^+. However, the diminution is ten times higher when the anion is $[TPB]^-$.

On the other hand, inspection of B parameter values (i.e. $B = \varepsilon_{EP}/\varepsilon_s$) points out that between 50 ºC and 180 ºC it increases 20 times for PBI@H[COSANE], about 40 times for PBI@Li[COSANE], 60 times for PBI@Na[COSANE] and around 10 times for PBI@Li[TPB] and PBI@Na[TPB], respectively. That means that the jump between the

sample permittivity ($\varepsilon_s \cong \varepsilon_\infty$) and electrode polarization permittivity ε_{EP} is higher in case of PBI@M[COSANE] (with M = H^+, Li^+, Na^+) than PBI@M'[TPB] (M' = Li^+, Na^+).

Considering that cation and anion have approximately equal mobility, we can write

$$\sigma_{dc} = nq\mu \qquad (5)$$

Where n is the carrier density, q the charge of a monovalent cation and μ the mobility. Taking into consideration that relaxation time τ is defined by $\tau=\varepsilon/\sigma_{dc}$ we can determine the mobility as[37]

$$\mu = \frac{qL^2}{4B\tau_{EP}kT} \qquad (6)$$

and then in view of the Nernst-Einstein equation we calculate the diffusion coefficient by mean of the expression

$$D = \frac{L^2}{4B\tau_{EP}} \qquad (7)$$

Finally, neglecting ion-ion interactions the free-ion density can be obtained combining eqn. (5), (6) and (7), obtaining

$$n = \frac{\sigma_{dc}}{q\mu} = \frac{\sigma_{dc}4B\tau_{EP}kT}{(qL)^2} \qquad (8)$$

Eqn (8) allows determining the average density of charge carriers from the values of the ionic conductivity previously determined, and from the values of diffusion coefficients calculated according to eqn. (7). Assuming the electrolyte is univalent we have estimated the values of diffusion coefficient and charge density for each sample from eqn (7) and (8), respectively. Our results are given in Table 3. A close inspection of Table 3 shows that the free ion number density increased for all samples when temperature rises. Inspection of Fig. 6 evidenced that conductivity can be correlated to the increase of free charge carrier density shown in Table 3. The increase of conductivity and concentration of free charge carriers may be due to the structural and morphological changes that occur in the PBI composite membranes. Guest molecules such as H[COSANE], Li[COSANE] and Na[COSANE] inside the matrix of PBI appear to be a determinant factor for the charge carrier density where the carrier density increases with increasing temperature

almost two orders of magnitude when comparing $[COSANE]^-$ with $[TPB]^-$. This increase could be related to the ion binding energy, which is function of distance between centres of pairs of ions, which in turn is related to the sizes of the ions and the dielectric constant of the medium. A comparison between the composite membrane of different ions with $[COSANE]^-$ shows that carrier densities of H[COSANE], Li[COSANE] are about one order of magnitude higher than Na[COSANE] which could be related to the ionic radii between the centres of pairs of $[COSANE]^-$ and H^+, Li^+ and Na^+, because, for example, this distance is 3.83 Å for lithium and 4.09Å for sodium ion, and then the binding energy, assuming that the same constant dielectric permittivity in both membranes, will be larger for the composite PBI@Li[COSANE] than for PBI@Na[COSANE].

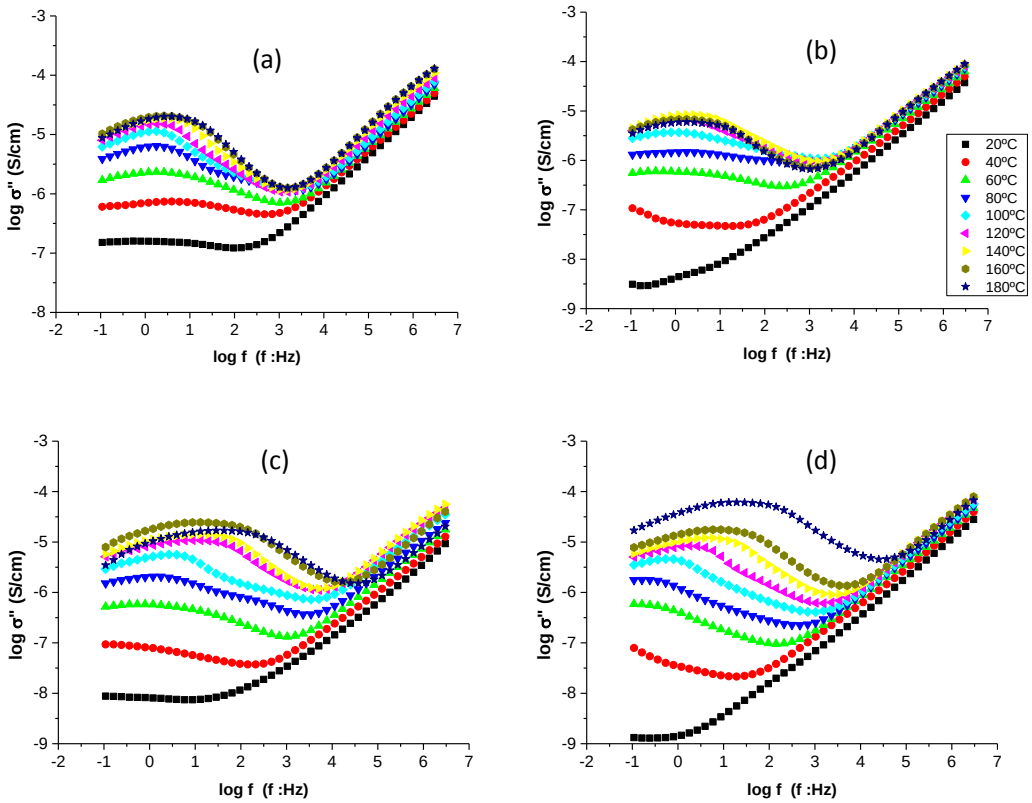

Fig. 9 Double logarithmic plot of imaginary part of the conductivity versus frequency for 20ºC (■), 40ºC (●), 60ºC (▲), 80ºC(▼), 100ºC (◆), 120ºC(◀), 140ºC (▶), 160ºC (⬢) and 180ºC (★). a) PBI@Li[COSANE], b) PBI@Na[COSANE], c) PBI@Li[TPB] and d) PBI@Na[TPB].

Fig. 9 shows a conductive process more important for samples with Li^+ than Na^+, both in the $[COSANE]^-$ and $[TPB]^-$ samples. The existence of two regions is also manifested in the Double logarithmic plot of imaginary part of the conductivity versus frequency, where

a broad relaxation peak appears, which shifts towards higher frequencies with increasing temperature. It can be observed that Li^+ has a significant conductivity at 20 ºC in $[COSANE]^-$ and $[TPB]^-$, whereas for Na^+ a significant conductivity starts around 30 ºC in both samples. The temperature dependence is also more pronounced for the Li^+ than for Na^+ samples, in agreement with the conductivity values obtained for both ions from Bode diagrams, which values were $1.7x10^{-6}$ S/cm at 30 ºC to $8.0x10^{-5}$ S/cm at 180 ºC for PBI@Li[COSANE], while this variation was $1.8x10^{-7}$ S/cm to $2.6x10^{-5}$ S/cm for PBI@Na[COSANE] for the same temperatures. On the other hand, the amount of carriers density determined from eqn (8) for both ions in the composite samples varies between 10^{21} and 10^{25} m^{-3} for PBI@Li[COSANE], and 10^{21} and 10^{23} m^{-3} for PBI@Na[COSANE] at 30 and 180 ºC, respectively.

When the values of the inverse Debye length can be obtained from the peaks of the loss tangent, the values of ε_s can be estimated. Eqn (9) provides an indirect method to calculate the static permittivity, ε_s. This method obeys to the equation of Anatoly Serguei,[26] where the permittivity can be expressed in function of the values f_{ON} and f_{Max} obtained from the curves of double logarithmic plot of σ" versus frequency, as

$$\varepsilon_s = \frac{\sigma_{dc}}{2\pi\varepsilon_0}\frac{f_{Max}}{f_{ON}^2} \qquad (9)$$

Fig. 9 shows the plots of double logarithmic of σ" versus frequency in the complete range of temperatures studied for PBI@Li[COSANE], PBI@Na[COSANE], PBI@Li[TPB] and PBI@Na[TPB]. In supplementary information we can see the plot obtained for PBI@H[COSANE]. (See Fig. S2).

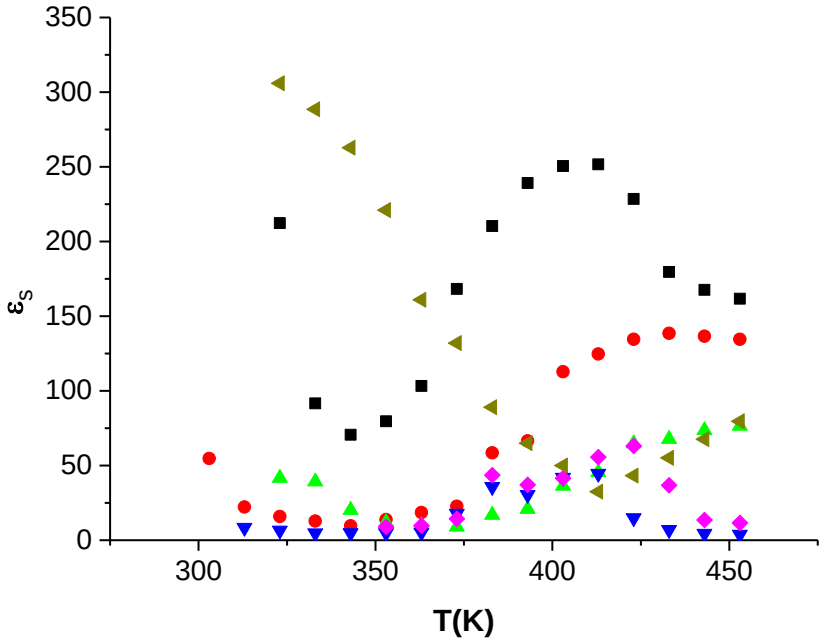

Fig. 10 Static permittivity of the samples in all the interval of temperatures calculated following the equation of Anatoly Serguei. (PBI@H[COSANE]) (■), (PBI@Li[COSANE]) (●), (PBI@Na[COSANE]) (▲), (PBI@Li[TPB]) (▼), (PBI@Na[TPB]) (◆). For comparison we also plotted the static permittivity for pristine PBI@ membrane (◀).

From Fig. 10 we have determined for each sample at each temperature, the frequency values of the onset (f_{ON}) and full development of electrode polarization (f_{MAX}), respectively. The determination of these values has permitted to find out the static permittivity following eqn (9). The results obtained are shown in Fig. 10. The dielectric constant was calculated indirectly using the equation of Anatoli Serguei, because plots of $\varepsilon'(\omega)$ do not contain clear plateaus from which we can determine ε_s (See Fig. S3). A close inspection of these results indicates that ε_s decreases, for the samples PBI@M[COSANE], (M= H^+, Li^+, Na^+) when the temperature increases until reaches a minimum value depending of ion type, then it increases until reaching the maximum value, which has been observed around 140 ºC in case of H^+ and around 160 ºC for Li and Na ions, quite similar to the solvent evaporation temperature. There is a subsequent reduction likely due to thermal randomization with increasing temperature, this is quite similar to what happens for samples of poly(ethylene oxide)-based sulfonated ionomer with Li^+ and Na^+ cations.[37] On the other hand, surprisingly high values of dielectric constant up to 100 ºC were found in the PBI@H[COSANE] in comparison with PBI@Li[COSANE] and

PBI@Na[COSANE]. Finally, the static permittivity was greater for membranes of PBI@M[COSANE] than PBI@M'[TPB].

4. CONCLUSIONS

The composite membranes of PBI@M[COSANE] (M = H^+, Li^+, Na^+) and PBI@M'[TPB] (M' = Li^+, Na^+) show high thermal stability and excellent physicochemical properties. The composite membranes exhibit higher water uptake and ionic conductivity than other membranes as Polybenzimidazol doped with HPSS. The conductivity of the composite membranes follows the trend σ(PBI@H[COSANE]) > σ(PBI@Na[COSANE]) > σ(PBI@Li[COSANE]) > σ(PBI@Na[TPB]) > σ(PBI@Li[TPB]) for temperatures up 100 ºC, showing that conductivities of composites at 150 ºC are higher than pristine PBI membranes, between one to two orders of magnitude depending on the type of ion. We have checked from the electrode polarization model a different method of Thrukhan theory to determine the diffusion coefficient and mobile ion concentration of a single-ion polymer electrolyte containing H^+, Li^+ and Na^+ cations. The methodology used in this work was the fit of tan δ = ε"/ε' versus frequency following the same procedure that before has been used by Klein and coworkers. High values of dielectric constant were found in all the samples. We are found that the dependence with temperature of diffusivity is more pronounced for the Li^+ than Na^+ samples in agreement with the conductivity values obtained for both ions from Bode diagrams. On the other hand, the amount of carriers density for Li^+ and Na^+ ions in the composite samples varying between 10^{21} and 10^{25} m^{-3} for PBI@Li[COSANE] and 10^{21} and 10^{23} m^{-3} in case of PBI@Na[COSANE] in all the range of temperatures studied.

The relaxation time of electrode polarization presents an opposite behavior in the case of the samples PBI@Li[COSANE] and PBI@Na[COSANE] than PBI@Li[TPB] and PBI@Na[TPB].

That means that the jump between the sample permittivity ($\varepsilon_s \cong \varepsilon_\infty$) and electrode polarization permittivity ε_{EP} is higher in case of PBI@M[COSANE] (with M = H^+, Li^+, Na^+) than PBI@M'[TPB] (M' = Li^+, Na^+).

ACKNOWLEDGEMENTS

We gratefully acknowledge to Spanish Ministerio de Economía y Competitividad (MINECO) for financial support by the ENE/2015-69203-R project and CTQ2016-75150-R project, and Generalitat de Catalunya (2014/SGR/149). I. Fuentes is enrolled in the PhD program of the UAB. The authors acknowledge Dr. Oscar Sahuquillo for technical assistance in TGA analysis.

REFERENCES

1. I. E. A. Statistics, IEA, Paris, France, 2016.

2. W. Li, J. R. Dahn, and D. S. Wainwright, *Science*, 1994, **264**, 1115-1117.

3. H. Lee, M. Yanilmaz, O. Toprakci, K. Fu, and X. Zhang, *Energy Environ. Sci.*, 2014, **7**, 3857-3886.

4. B. Anothumakkool, A. Torris AT, S. Veeliyath, V. Vijayakumar, M. V. Badiger, and S. Kurungot, *ACS Appl. Mater. Interfaces*, 2016, **8**, 1233-1241.

5. C. Huang, J. Zhang, H. J. Snaith, and P. S. Grant, *ACS Appl. Mater. Interfaces*, 2016, **8**, 20756-20765.

6. Y. Wang, K. S. Chen, J. Mishler, S. C. Cho, and X. C. Adroher, *Applied Energy*, 2011, **88**, 981-1007.

7. A. Kraytsberg and Y. Ein-Eli, *Energy Fuels*, 2014, **28**, 7303-7330.

8. F. Lufrano, V. Baglio, P. Staiti, and V. Antonucci, *J. Power Sources*, 2013, **243**, 519-534.

9. N. Awang, A. F. Ismail, J. Jaafar, T. Matsuura, H. Junoh, M. H. D. Othman, and M. A. Rahman, *React. Funct. Polym.*, 2015, **86**, 248-258.

10. S. P. Nunes, B. Ruffmann, E. Rikowski, S. Vetter, and K. Richau, *J. Membr. Sci.*, 2002, **203**, 215-225.

11. D. H. Jung, S. Y. Cho, D. H. Peck, D. R. Shin, and J. S. Kim, *J. Power Sources*, 2003, **118**, 205-211.

12. M. K. Song, S. B. Park, Y. T. Kim, K. H. Kim, S. K. Min, and H. W. Rhee, *Electrochim. Acta*, 2004, **50**, 639-643.

13. Z. Gaowen and Z. Zhentao, *J. Membr. Sci.*, 2005, **261**, 107-113.

14. V. R. Hande, S. K. Rath, S. Rao, and M. Patri, *J. Membr. Sci*., 2011, **372**, 40-48.

15. G. K. Shimizu, *J. Solid State Chem*., 2005, **178**, 2519-2526.

16. Q. Li, R. He, J. O. Jensen, and N. J. Bjerrum, *Chem. Mater*., 2003, **15**, 4896-4915.

17. J. A. Hurd, R. Vaidhyanathan, V. Thangadurai, C. I. Ratcliffe, I. L. Moudrakovski, and G. K. Shimizu, *Nat. Chem*., 2009, **1**, 705-710.

18. S. S. Araya, F. Zhou, V. Liso, S. L. Sahlin, J. R. Vang, S. Thomas, X. Gao, C. Jeppesen, and S. K. Kaer, *Int. J. Hydrog. Energy*, 2016, **41**, 21310-21344.

19. I. Fuentes, A. Andrio, F. Teixidor, C. Viñas, and V. Compañ, *Phys. Chem. Chem. Phys.*, 2017, **19**, 15177-15186.

20. K. A. Mauritz and R. B. Moore, *Chem. Rev*., 2004, **104**, 4535-4586.

21. G. Alberti, R. Narducci, and M. Sganappa, *J. Power Sources*, 2008, **178**, 575-583.

22. P. R. Sukumar, W. Wu, D. Markova, O. Unsal, M. Klapper, and K. Mullen, *Macromol. Chem. Phys*., 2007, **208**, 2258-2267.

23. H. Pu, L. Liu, Z. Chang, and J. Yuan, *Electrochim. Acta*, 2009, **54**, 7536-7541.

24. J. C. Dyre and T. B. Schroder, *Rev. Mod. Phys*., 2000, **72**, 873.

25. B. Roling, C. Martiny, and S. Bruckner, *Phys. Rev. B*, 2001, **63**, 214203.

26. A. Serghei, M. Tress, J. R. Sangoro, and F. Kremer, *Phys. Rev. B*, 2009, **80**, 184301.

27. H. Pu, L. Lou, Y. Guan, Z. Chang, and D. Wan, *J. Membr. Sci*., 2012, **415**, 496-503.

28. S. Tominaka and A. K. Cheetham, *RSC Adv*., 2014, **4**, 54382-54387.

29. P. Barbosa, N. C. Rosero-Navarro, F. N. Shi, and F. M. Figueiredo, *Electrochim. Acta*, 2015, **153**, 19-27.

30. C. Krause, J. R. Sangoro, C. Iacob, and F. Kremer, *J. Phys. Chem. B*, 2009, **114**, 382-386.

31. A. Rivera and E. A. Rossler, *Phys. Rev.B*, 2006, **73**, 212201.

32. T. S. Sorensen and V. Compañ, *J. Chem. Soc. Faraday Trans*., 1995, **91**, 4235-4250.

33. T. S. Sorensen, V. Compañ, and R. Diaz-Calleja, *J. Chem. Soc. Faraday Trans*., 1996, **92**, 1947-1957.

34. A. Munar, A. Andrio, R. Iserte, and V. Compañ, *J. Non-Cryst. Solids*, 2011, **357**, 3064-3069.

35. J. R. Macdonald, *Phys. Rev*., 1953, **92**, 4.

36. R. Coelho, *Revue Phys. Appl*., 1983, **18**, 137-146.

37. R. J. Klein, S. Zhang, S. Dou, B. H. Jones, R. H. Colby, and J. Runt, *J. Chem. Phys.*, 2006, **124**, 144903.

38. R. Coelho, *J. Non-Cryst. Solids*, 1991, **131**, 1136-1139.

39. M. Jonsson, K. Welch, S. Hamp and M. Stromme, *J. Phys. Chem. B*, 2006, **110**, 10165-10169.

40. T. M. W. J. Bandara, M. A. K. L. Dissanayake, I. Albinsson, and B. E. Mellander, *Solid State Ion.*, 2011, **189**, 63-68.

41. S.D. Pasini Cabello, S. Molla, N. A. Ochoa, J. Marchese, E. Gimenez, and V. Compañ, *J. Power Sources*, 2014, **265**, 345-355.

42. A. Garcia-Bernabe, A. Rivera, A. Granados, S. V. Luis, and V. Compañ, *Electrochim. Acta*, 2016, **213**, 887-897.

43. V. Compañ, S. Molla, E. G. Verdugo, S. V. Luis, and M. I. Burguete, *J. Non-Cryst. Solids*, 2012, **358**, 1228-1237.